Structure, Vol. 11, 165–174, February, 2003, ©2003 Elsevier Science Ltd. All rights reserved. PII S0969-2126(03)00008-X

A Novel Protein Fold and Extreme Domain Swapping in the Dimeric TorD Chaperone from *Shewanella massilia*

Samuel Tranier,[1] Chantal Iobbi-Nivol,[2] Catherine Birck,[1,3] Marianne Ilbert,[2] Isabelle Mortier-Barrière,[1] Vincent Méjean,[2] and Jean-Pierre Samama[1,3,*]

[1]Groupe de Cristallographie Biologique
Institut de Pharmacologie et Biologie Structurale
205 route de Narbonne
31077 Toulouse Cedex
France

[2]Laboratoire de Chimie Bactérienne
Institut de Biologie Structurale et Microbiologie
Centre National de la Recherche Scientifique
13402 Marseille Cedex 20
France

Summary

TorD is the cytoplasmic chaperone involved in the maturation of the molybdoenzyme TorA prior to the translocation of the folded protein into the periplasm. The X-ray structure at 2.4 Å resolution of the TorD dimer reveals extreme domain swapping between the two subunits. The all-helical architecture of the globular domains within the intertwined molecular dimer shows no similarity with known protein structures. According to sequence similarities, this new fold probably represents the architecture of the chaperones associated with the bacterial DMSO/TMAO reductases and also that of proteins of yet unknown functions. The occurrence of multiple oligomeric forms and the chaperone activity of both monomeric and dimeric TorD raise questions about the possible biological role of domain swapping in this protein.

Introduction

Trimethylamine N-oxyde (TMAO) is widely distributed in marine fishes and mollusks, where it is assumed to act as an osmoprotector in living tissues. In decaying organisms, TMAO is reduced to the nauseous trimethylamine (TMA) and plays an important role in tissue spoilage. This reduction is mainly mediated by the bacterial species of the fish flora, such as *Shewanella* and *Vibrio* species, which use TMAO as an exogeneous electron acceptor for anaerobic respiration [1, 2]. TMAO-reducing activity was also observed in photosynthetic bacteria (*Rhodobacter* species) and, more surprisingly, in most enterobacteria [3–5]. The dedicated respiratory system is encoded by the *TorCAD* and *TorECAD* operons in *Escherichia coli* and *Shewanella* species, respectively [1, 6, 7].

The proteins encoded by the *torA*, *torC*, and *torD* genes have been characterized. The mature TorA enzyme is a periplasmic TMAO-specific reductase [8] that belongs to the family of DMSO-TMAO molybdoenzymes. The three-dimensional structure of the protein from *S. massilia*, a marine bacterium responsible for fish tissue decay, illustrated that the 798 residues fold into four domains organized around the molybdenum cofactor [9]. This periplasmic enzyme operates together with the c-type cytochrome TorC, which is anchored to the innermembrane and shuttles electrons from the membranous menaquinones to the reductase. The tetrahemic N-terminal domain of TorC binds to TorA and transfers electrons to the monohemic C-terminal domain, which ultimately provides them to the reductase [10]. Interestingly, the immature C-terminal domain of apocytochrome TorC downregulates the *tor* operon by binding to the sensor region of TorS, the histidine kinase of the TorS/TorR phosphorelay that strictly controls expression of the operon in response to TMAO availability [11].

In *E. coli*, the absence of TorD leads to a significant decrease in the amount of TorA, and in vitro experiments showed that TorD binds both the TorA enzyme and its precursor form [12]. It was proposed that TorD acts as a private chaperone of the reductase, and recent experiments indicate that TorD allows efficient maturation of TorA (M. Ilbert and C.I.-N., in preparation). This process, which involves insertion of the molybdopterin cofactor, is a prerequisite event for the translocation of the protein into the periplasm by the twin-arginine translocation (TAT) system, which transports TorA as a folded holoprotein [13, 14]. The targeting of TorA to the TAT system is mediated by a specific amino-terminal signal peptide that exhibits the consensus motif S/T-R-R-X-F-L-K, which is also found in a variety of periplasmic redox enzymes [15].

The TorD protein from *S. massilia* interacts specifically with its cognate reductase, TorA. The chaperone is 33% identical in sequence to the *E. coli* ortholog and displays multiple and stable oligomeric forms. The monomeric and dimeric species of the protein were characterized by analytical ultracentrifugation, and interconversion between these forms required conditions that destabilize the native fold of the proteins [16]. The X-ray structure of the dimeric TorD protein reported here was solved at 2.4 Å resolution by the MAD method. The protein displays a dumbbell-like shape and reveals extreme domain swapping between the two subunits. The all-helical architecture of the globular domain in the dimer and the geometry of the motif constituting the open interface region show no similarity with reported protein structures. Structure analysis, together with small-angle scattering data, suggests that the globular domain in the dimer illustrates the structure of the monomeric species of the protein. According to sequence similarities, the fold of the TorD protein likely represents the architecture of the chaperones associated with the DMSO-TMAO bacterial reductases.

*Correspondence: samama@igbmc.u-strasbg.fr
[3]Present address: Département de Génomique et de Biologie Structurale, IGBMC, 1 rue Laurent Fries, BP 10142, 67404 Illkirch, France

Key words: TorD; chaperone; 3D domain swapping; twin-arginine translocation; X-ray structure; molybdoenzyme

Table 1. Data Collection and MAD Phasing Statistics

	Native	Edge λ_1 = 0.9787 Å	Peak λ_2 = 0.9785 Å	λ_3 = 0.9537 Å
Resolution (Å)	19.61–2.42	54.23–2.40	54.23–2.40	54.23–2.4
Reflections Measured/unique	108,921/21,290	136,737/23,612	214,824/23,643	85,570/23,239
Completeness %	90.3 (81.6)[e]	100 (99.7)	99.8 (98.8)	98.7 (98.9)
I/σ	11 (2.8)[e]	12.8 (3.7)	11 (4.2)	14 (3.6)
R_{sym}[a]	0.040 (0.368)[e]	0.041 (0.168)	0.046 (0.168)	0.033 (0.177)
R_{ano}[b]	—	0.030	0.047	0.036
f′/f″ (e−)[c]	—	−9.5/2.3	−8.1/5.5	−4.5/3.5
Z score/FOM[d]	—		28/0.56	

[a] $R_{sym} = \Sigma\Sigma|<I> - I_i|/\Sigma\Sigma I_i$.
[b] $R_{ano} = \Sigma|<I^+> - <I^->|/\Sigma|<I^+> + <I^->|$.
[c] Values of anomalous scattering factors, as refined by SOLVE, used for phasing.
[d] Phasing statistics provided by the program SOLVE; FOM, figure of merit.
[e] Outer resolution shell in parentheses.

Results

Structure Determination

All methionines, except the cleaved N-terminal methionine, in the sequence of TorD from *S. massilia* were substituted by SeMet, according to mass spectrometry. The dimeric species of the TorD protein crystallized in the orthorhombic space group $P2_12_12_1$, with one dimer in the asymmetric unit, and the structure was determined to 2.4 Å resolution from MAD phasing at the selenium K absorption edge. Only four (SeMet-143^{su1}, SeMet-114^{su2}, SeMet-139^{su2}, and SeMet-143^{su2}) of the six SeMet residues present in the dimer were found by SOLVE [17] and used for phasing (Table 1). The two scattering atoms that escaped the automatic search, SeMet-114^{su1} and SeMet-139^{su1}, were found to be located only 5 Å away from other SeMet residues. They were nevertheless well defined in the initial electron density map. The final model comprises 3117 nonhydrogen atoms from the TorD dimer, two DTT molecules, and 144 water molecules. The crystallographic R and R_{free} values were 0.224 and 0.255, respectively (Table 2). The average refined B factors (Table 2) were in excellent agreement with the value (41.5 Å^2) determined from a Wilson plot analysis of the diffracted intensities.

No electron density could be assigned to residues 1–3, 87–88, and 99–104 in one subunit or to residues 1–4, 86–88, and 99–107 from the other subunit. The recombinant protein carried, in addition to the natural 209 residues, two additional amino acids and 6 histidine residues at the C terminus. Residues 209–215 from one subunit contribute to crystal packing. A few solvent-exposed side chains were disordered, and residues Q28^{su1}, E48^{su2}, C79^{su1,su2}, and E131^{su2} had alternate conformations. The electron density map (Figure 1) suggested a correction of the amino acid sequence (H8P, F147C, and F163V) of TorD from *S. massilia* [1]; this was confirmed by gene sequencing. According to PROCHECK [18], 93.5% of the residues belong to the most favorable areas in the Ramachandran plot. The conformations of the other residues are in allowed regions.

Table 2. Refinement Statistics

Resolution (Å)	2.4
R factor (%)	22.4
R_{free} (%)	25.5
Rmsd bond lengths (Å)	0.007
Rmsd bond angles (°)	1.2
Rmsd dihedral angles (°)	19.7
Rmsd improper angles (°)	0.87
Mean B factor (Å^2)	43.8
Rmsd B, bonds (Å^2)	
Main chain atoms	1.0
Side chain atoms	2.8
Rmsd B, angles (Å^2)	
Main chain atoms	1.8
Side chain atoms	4.0
Number of protein atoms	3117
Number of heteroatoms	114 H_2O
	2 DTT

Overall Structure

The TorD dimer displays an all-helical architecture that comprises 69.6% of the amino acids and reveals extreme domain swapping between the two subunits (Figure 2). The dimeric protein displays a dumbbell-like shape, with molecular 2-fold symmetry. Each globular module contains ten α helices and two small 3_{10} helices (Figure 3) and results from the association of the N-terminal moiety from one subunit (residues 1–126) with the C-terminal moiety from the other subunit (residues 133–209). The module seems organized around a helix bundle core formed by the first helix of one subunit (H_1^{su1} residues 7–22) and by the helices provided by the whole C-terminal moiety from the other subunit: H_7^{su2} (residues 136–149), H_8^{su2} (residues 152–163), H_9^{su2} (residues 167–174), and H_{10}^{su2} (residues 182–209) (Figure 3). This helix bundle is surrounded by the remaining part of the first subunit: H_2^{su1} (residues 27–34), H_3^{su1} (residues 36–46), H_4^{su1} (residues 52–64), H_5^{su1} (residues 68–82), and H_6^{su1} (residues 108–121) (Figure 3). The molecular interface (C interface) between the swapped N- and C-terminal moieties buries 4500 Å^2 from solvent. No protein structure with a similar topology has been found in the protein structure database with DALI [19].

Networks of polar interactions occur at two important regions of the C interface. The first area involves the N- and C-terminal ends of the protein, tightly held at one edge (H1^{su1}, H8^{su2}, and H10^{su2}) of the helix bundle core (Figure 3). Asp-197, at the C-terminal part of helix H10^{su2}, forms a salt bridge and a hydrogen bond interaction with Arg-10 and Tyr-14, respectively, from helix H1^{su1}. Arg-10 is also hydrogen bonded to the side chain

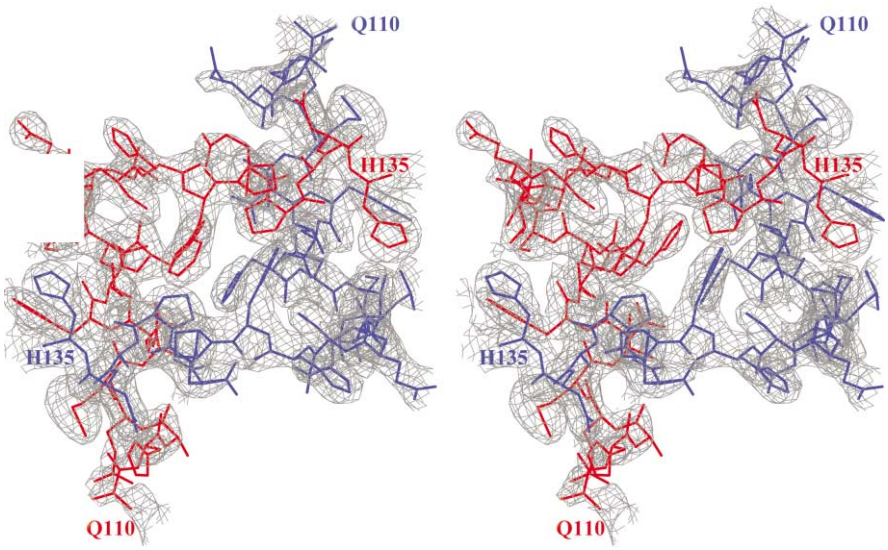

Figure 1. Stereo View of the Final $2F_o - F_c$ Electron Density Map, Contoured at 1 σ above the Mean, in the Crossover and Dimerization Region
Residues 108–135 from subunit 1, blue; residues 108–135 from subunit 2, red.

of Gln-155, located at the N-terminal part of helix $H8^{su2}$. The second area is found at the edge of the crossover region. A network of polar interactions involves His-134, His-135, Leu-136, and Ala-137 from the same subunit and Pro-92, Tyr-93, Ala-94, Ser-95, and His-111 from the other subunit (Figure 3). This area comprises invariant residues in the TorD orthologs (Figure 4) and seems critical because these interactions define the position of the first residues (134–137) of the C-terminal moiety within the N-terminal moiety of the protein. It brings the carbonyl oxygen of Ala-137 from helix $H7^{su2}$ within hydrogen bond distance of Ser-18 from $H1^{su1}$ (Figure 3), which may be an important anchor point for the formation of the helix bundle core.

The two polypeptide chains are highly intertwined, and the dimerization element involves the H6 helix (residues 108–121), the loop 122–124, and the polypeptide stretch 125–135, the direction of which is orthogonal to the axis of helix H6 (Figure 5). There are 18 polar residues within the 28 amino acids defining this motif, which is duplicated by the molecular 2-fold symmetry. The two globular modules are connected by residues 125–135 from each subunit, which form two adjacent, extended, antiparallel peptide stretches. The molecular 2-fold axis is nearly perpendicular to the average plane defined by these stretches, running between the two Phe-129 side chains, which are at van der Waals distance to each other (Figure 5). On one side of this plane, at the edge of the crossover region, Tyr-93 and Phe-129 from the same subunit and Pro-130, Pro-132, and His-135 from the other subunit are in close vicinity (Figure 5). The hydroxyl group of Tyr-93 is at hydrogen bond distance to one nitrogen atom from the buried His-135 side chain. On the other side of the plane defined by the two peptide stretches, Asp-134 from one subunit and His-111 from helix 6 of the other subunit are hydrogen bonded (2.7 Å). The C-terminal parts of the H6 helix from each subunit are proximal and run antiparallel in the swapped dimer. As a consequence, Glu-116, His-119, Gln-120, and their symmetry-related counterparts come in close vicinity (Figure 5). The two imidazole rings are stacked on each other at a distance of 4 Å, and each side chain is hydrogen bonded to the carboxylate group of Glu-116 from the other subunit (Figure 5). The interactions described in this paragraph define the open interface region [20] generated by 3D domain swapping and bury 440 $Å^2$ from solvent.

The TorD Protein Family

A Psi-Blast search in the sequence database with the amino acid sequence of TorD from *Shewanella massilia* identified proteins with significant sequence similarities. Some of these proteins from other bacterial species are orthologs of TorD according to the conservation of the *tor* operon in the corresponding genomes. In decreasing order of sequence identity, TorD proteins were found in *Shewanella oneidensis* (71.8%), *Vibrio cholerae* (39.3%), *E. coli* (34.7%), *Salmonella thyphi* CT18 (33.5%), and *Pasteurella multocida* (29.8%). TorD homologs occur in *Haemophilus influenzae* (YnfI, 27.5%), *E. coli* (YnfI or DmsD, 21.1%) [21], and *Rhodobacter capsulatus* (DorD, 25.6%) [22]. A protein with no known function, YcdY, was found in *E. coli* and *Haemophilus influenzae* (21% and 27.5% identity, respectively). All the proteins identified in this search are made of approximately 200 amino acids, and a multiple sequence alignment was performed on the basis of the structure of the *S. massilia* protein (Figure 4). The overall sequence identity between these proteins and the finding that the few invariant or highly conserved hydrophobic residues (Leu-17, Phe-21, Leu-81, Phe-82, Leu-136, Leu-140, Trp-166, Leu-167, Phe-170, Tyr-183, and Leu-189) constitute a hydrophobic core in the globular domain (Figure 3) suggest that these proteins share the same all-helical three-dimensional fold.

The six ORFs assigned as TorD orthologs display in-

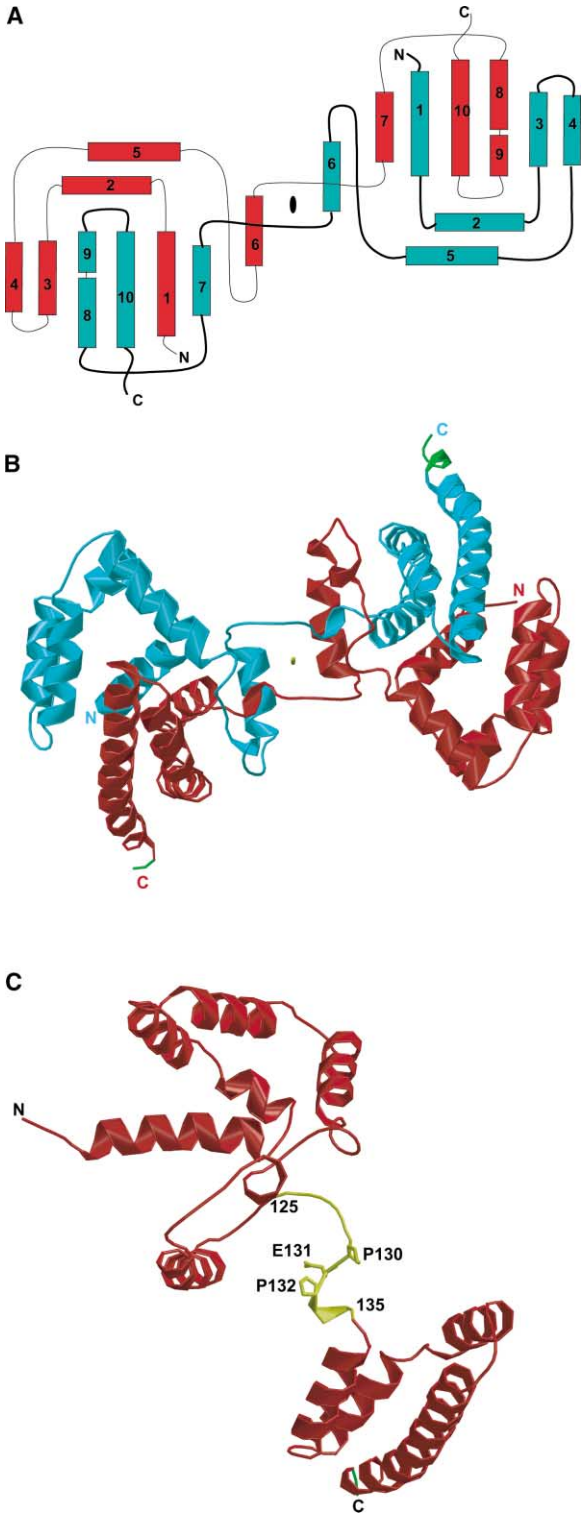

Figure 2. The TorD Structure

(A) Topology of the TorD dimer with one monomer in green and the other in red. Helices are represented by cylinders and numbered sequentially, and the connecting loops are represented with a different line thickness for each monomer.

(B) Ribbon representation of the TorD dimer with the same color code.

(C) Ribbon representation of one monomer within the dimer. The PEP sequence (residues 130–132) shown within the crossover polypeptide stretch (residues 125–135).

variant residues at positions 72–77 in helix H5, in addition to the 92–95 and 131–138 regions discussed above as forming a key area in the globular domain. Residues 72–77 and 92–95/131–138 generate acidic areas (A) and polar surfaces (P), respectively, on the TorD dimer. A Grasp [23] representation (Figure 6) illustrated that a 60 Å-long depression is bordered by all four surfaces, whereas two of them (one A and one P) face another large cavity in the swapped dimer. In monomeric TorD, which corresponds to one globular domain on Figure 6, the A and P surfaces are nearly contiguous along a convex surface.

Discussion

Domain Organization

The spatial organization of the 209 amino acids of the TorD monomer within the dimer (Figure 2) does not represent a stable fold. This structure is made of two separated domains and exposes several hydrophobic residues to solvent. From a structural viewpoint, this "open" monomer may represent a folding intermediate that could lead to the several molecular forms of the protein. Indeed, formation of the monomer versus the swapped dimer from the "open" structure seems to depend only on the conformation of the polypeptide stretch 125–135. The extended conformation favors domain swapping, whereas a loop conformation of the peptide would bring the C-terminal domain back into the N-terminal moiety and result in a monomeric protein essentially represented by the globular module in the swapped dimer (Figure 3). This proposal is supported by the excellent fit between the diffusion data calculated from the coordinates of the globular module and the small-angle X-ray-scattering (SAXS) data measured for the TorD monomer (Figure 7). SAXS experiments were also conducted with the dimeric protein and provided a similar agreement between the measured diffusion data and those calculated from the current X-ray structure (Figure 7).

The proposal that the fold of the monomer is represented by that of the globular domain in the swapped dimer underlies the conservation of the interdomain interface (C interface) in the two structures. This conservation is supported by the biochemical studies, which showed that acidic pH similarly disrupts the native monomeric and dimeric TorD structures. The polypeptide chain adopts a nonnative fold in these conditions [16]. According to the X-ray structure, an important contribution to the stability of the C interface is provided by two polar networks, and we propose that protonation at acidic pH of the two carboxylate side chains (Asp-134 and Asp-197) facing two positively charged residues, His-111 and Arg-10, respectively, and, possibly, of the buried histidine 135 (Figure 3) should destabilize this interface and favor the open monomer over the monomeric and swapped oligomeric structures.

Role of TorD Chaperones

The finding of several molecular species for the *S. massilia* protein raises questions about the general occurrence of 3D domain swapping in this protein family and

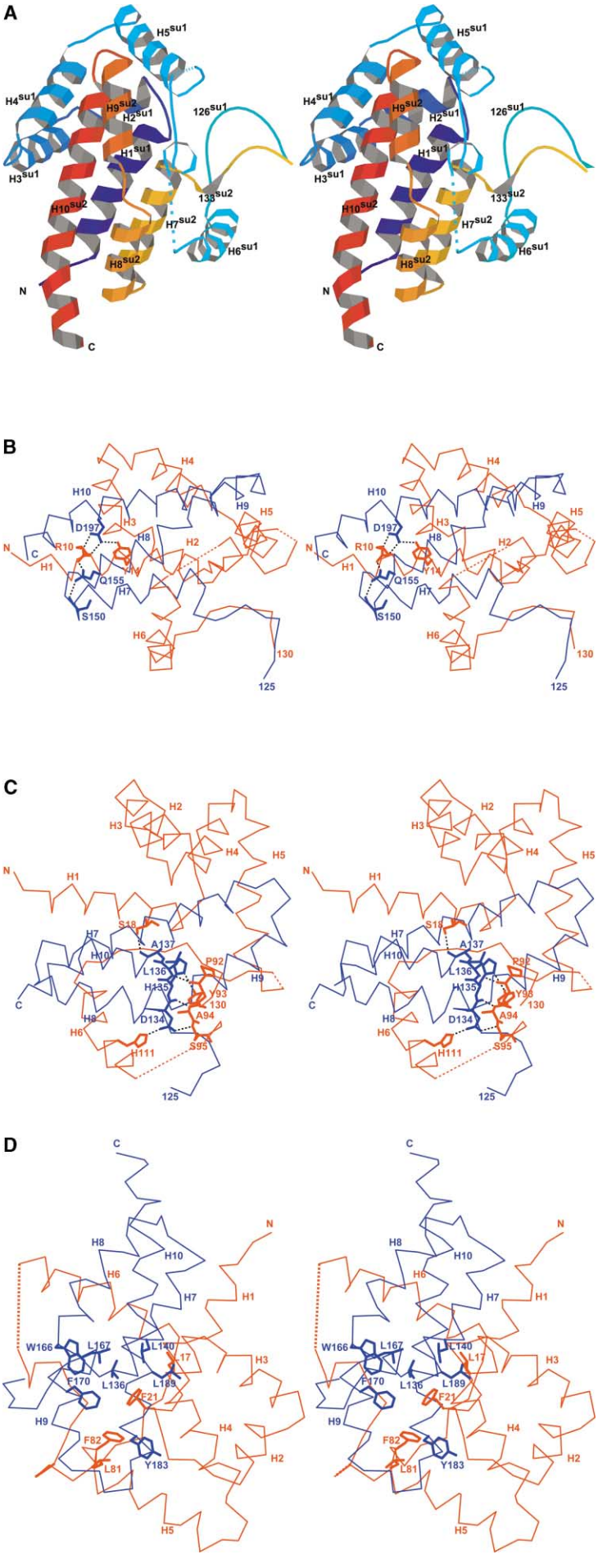

Figure 3. Molecular Interface in the Globular Module of the TorD Dimer

(A) Stereo view of the globular module within the dimer. Subunit 1 is colored from dark blue (N terminus) to green (residue 126); subunit 2 is colored from yellow (residue 133) to red (C terminus). The dotted line indicates a loop region with undefined electron density.

(B) Stereo view illustrating the polar interactions at the C interface and occurring at one edge of the helix bundle core. The CA traces of subunits 1 and 2 are shown in red and blue, respectively.

(C) Stereo view of the network of polar interactions involving invariant residues in the TorD family and stabilizing the C interface. The CA traces of subunits 1 and 2 are shown in red and blue, respectively.

(D) Stereo view illustrating the hydrophobic core in the globular module. These residues are invariant in the TorD family.

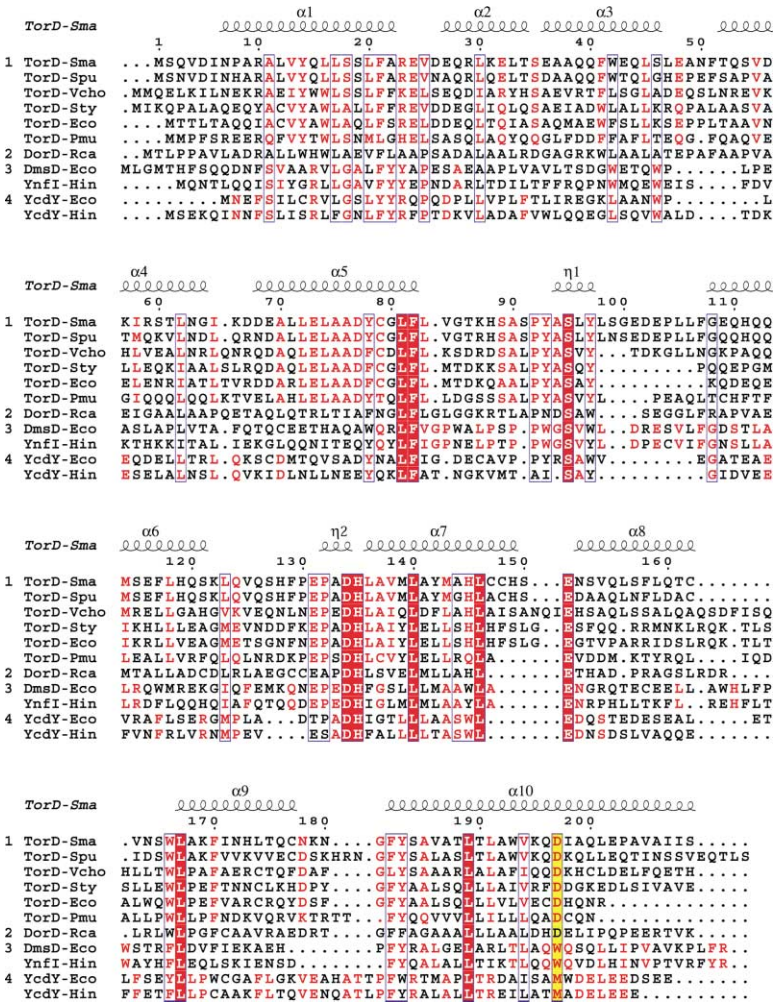

Figure 4. Structure-Based Sequence Alignment of the TorD Protein Family

The sequence identity between any two of these proteins is above 21%. The proteins from groups 1, 2, and 3 are TorD orthologs. The secondary structure elements for the TorD chain were calculated with DSSP [48]. The picture was created with ESPrit [49].

the possible biological role for domain swapping in TorD.

Three TorD orthologs carry the PEP sequence at positions 130–132, three others display the xEP sequence (Figures 2 and 4), and the conformation of the polypeptide stretch 125–135 likely determines formation of the monomer versus swapped oligomers. The PEP sequence is found in p13^{suc1}, where it was shown that the partition between the monomer and swapped dimers was only controlled by these two proline residues [24]. However, a large diversity in sequence of the hinge region was documented in proteins that undergo domain swapping, and the occurrence of a single proline in this region is common [25]. The occurrence of 3D domain swapping in all TorD proteins remains an open question but deserves further investigation because a relationship between 3D domain swapping and functional properties has been established in several cases. For most proteins, only one molecular form is biologically active. Regulation of cdk2 activity is only mediated by the monomeric species [26], and domain swapping in T4 endonuclease VII is mandatory for generating a functional protein with DNA binding and cleavage activity [27]. In diphteria toxin, [28] domain swapping and intoxication pathways are related processes. It was proposed that the transition from closed to open monomer, which leads to the oligomeric translocation assembly, is stimulated upon binding of the toxin monomer to the heparin binding epidermal growth factor, the cell surface target of the toxin [29]. In some cases, 3D domain swapping extends functionality. An additional dinucleotide binding site for allosteric regulation is generated in bovine seminal ribonuclease [30], and a large amphipathic binding site for pyrazine or carvone is created in bovine odorant binding protein [31]. It was previously established from genetic investigations that TorD is required prior to cofactor incorporation in the precursor TorA protein, and surface plasmon resonance measurements indicated formation of a protein complex between TorD and TorA [12]. Experiments in progress now demonstrate that TorD allows efficient maturation of the apoprecursor of TorA and that both the monomeric and dimeric forms of TorD facilitate molybdenum cofactor insertion in the apoprecursor (M. Ilbert and C.I.-N., in preparation). These data shed light on the mechanism of action of TorD as chaperone of TorA and suggest that domain swapping, if it occurs in vivo, may not be implicated in the modulation of this function.

This chaperone activity is critical because TorA is exported by the twin-arginine translocation system as

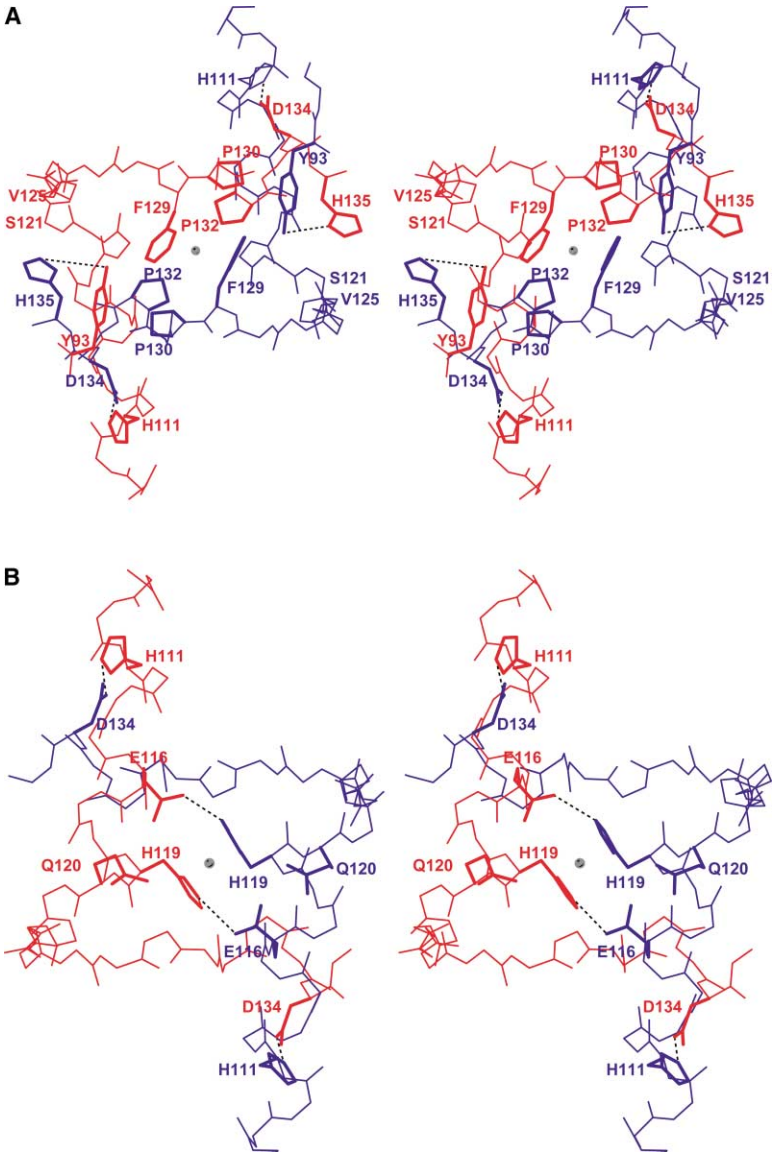

Figure 5. Stereo Views of the Open Interface and Dimerization Region Mediated by Residues 108–135 from Subunits 1 and 2

Residues 108–135 from subunit 1, blue; residues 108–135 from subunit 2, red. The molecular 2-fold axis is perpendicular to the plane of the figure.

(A) View from one side of the average plane defined by the stretch 125–135.

(B) View from the other side of this plane.

a folded holoprotein [32]. This is a basic feature of this export pathway, fundamentally distant from any system yet studied, which recognizes signal peptides carrying the characteristic sequence motif (S/T)-R-R-x-F-L-K [15]. Cofactor incorporation and protein targeting must therefore be coordinated in the translocation process, and it was suggested that the system could contain elements for proofreading before export is attempted [33]. Along this line, it was proposed that the signal peptide may be bound by an accessory protein that attaches itself to the apoform of the protein and may only be released after cofactor insertion [13]. It is now possible to state, on the basis of the functional and biochemical results reported above, that TorD fulfils the last two requirements. The affinity of the signal peptide of TorA for TorD has not been evaluated, but it was shown that the TorD homolog DmsD (Figure 4) binds the twin-arginine leader sequences of DmsA and TorA [21], two molybdopterin-containing reductases with significant sequence similarities. It is therefore possible that the acidic patch revealed by the X-ray structure of TorD (Figure 6) may sequester the basic S/T-R-R-X-F-L-K motif within the TorA-TorD complex that favors molybdenum cofactor acquisition. This possibility would support the proposal of proofreading and would confer to the TorD protein a function in the process of export mediated by the TAT system.

The knowledge about the original fold of TorD provides a new framework in which to investigate the mechanism of maturation and export of the TorA molybdoenzyme family.

Biological Implications

A variety of bacterial periplasmic redox enzymes are exported as folded holoproteins by the recently discovered twin-arginine translocation system. The best-documented enzyme with respect to export by the TAT machinery is TorA, a trimethylamine N-oxyde-specific reductase. This protein is part of the respiratory system

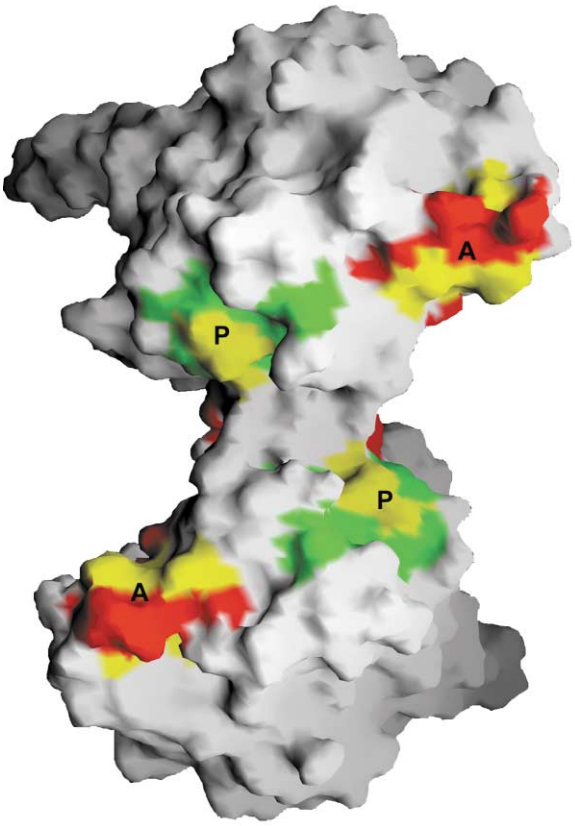

Figure 6. Grasp Representation of the Polar and Acidic Areas Generated by Invariant Residues in the TorD Protein Family Mapped on the Surface of the Structure of the TorD Dimer

P, polar; A, acidic.

encoded by the *torEACD* operon in *Shewanella massilia*, a bacterium responsible for fish tissue decay. TorD is the cytoplasmic chaperone of TorA and allows maturation of the enzyme, a prerequisite event for translocation of the enzyme into the periplasm.

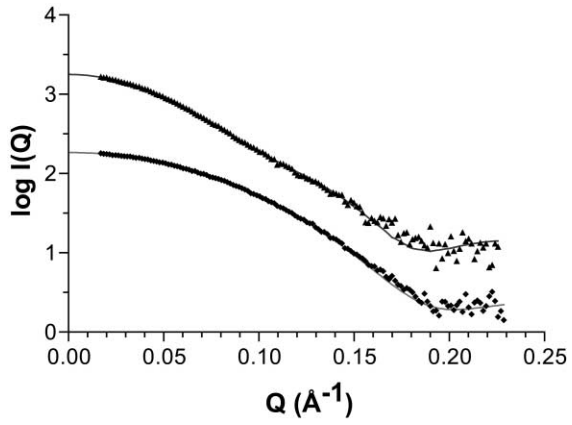

Figure 7. Comparison of the Scattering Data Measured by SAXS Experiments and Calculated from the X-Ray Structure

Experimental data (triangle) and data calculated with CRYSOL [47] for the TorD dimer. Experimental data (square) for the TorD monomer and calculated scattering data for one globular domain within the dimer (black curve).

TorD from this bacterium forms multiple oligomeric species, and the crystal structure of dimeric TorD reveals extreme domain swapping between the two subunits. The dimer displays a dumbbell-like shape, and the all-helical architecture of the globular module within the intertwined dimer shows no similarity with known protein structures. According to sequence and structure analysis, this new fold defines a family of putative chaperones from various bacterial species and includes proteins of yet unknown functions.

Both monomeric and dimeric TorD facilitates molybdenum cofactor incorporation and maturation of the precursor apo-TorA enzyme. These experiments suggest that domain swapping in TorD preserves a significant extent of the surface of the protein that mediates the formation of the TorD-TorA complex, observed by surface plasmon resonance. These data may also indicate that domain swapping, if it occurs in vivo, does not seem to be implicated in the modulation of the chaperone function. The structural, biochemical, and functional data presented in this report provide a new framework in which to study the maturation of molybdoenzymes and raise the possibility that TorD may have a complementary function of proofreading before transport of TorA is attempted.

Experimental Procedures

Expression and Purification

The *torD* gene of *S. massilia* was amplified from chromosomal DNA by PCR with primers SMD1 (5′-TTTCCATATGAGTCAAGTCGATAT CAACCACGC-3′), which corresponds to an NdeI site followed by the 5′ coding sequence of *torD*, and SMD2 (5′-TTTCTCGAGGC TAATTATCGCCACAGCGGGTTC-3′), which corresponds to an XhoI site followed by a sequence encoding the complementary sequence of the 3′ end of *torD*. The purified PCR product was digested by both restriction enzymes and ligated into the appropriate cloning sites of the expression vector, pet-22b (NOVAGEN), to give plasmid pet-TorD, which allows production of C-terminal His-tagged TorD protein. The absence of mutation was checked by DNA sequencing.

The recombinant vector was transformed into *E. coli* strain BL21(DE3)pLysS. Bacteria were grown at 37°C in Lenox broth medium supplemented with 100 μg ml^{-1} ampicillin and 35 μg ml^{-1} chloramphenicol to an OD_{600nm} of 0.7. Expression of the gene *torD* was induced by the addition of 0.5 mM IPTG (isopropyl β-D-thiogalactopyranoside) for 4 hr. Cells were harvested by centrifugation at 4500 × g for 20 min, resuspended in lysis buffer (20 mM sodium phosphate [pH 7.6], 500 mM NaCl, 1 mM DTT, 150 U benzonase (Merck), 10 μg ml^{-1} leupeptin, pepstatin, and TPCK, and 0.1 mM PMSF), and disrupted by sonication. The insoluble material was removed by centrifugation at 9000 × g for 2 hr.

All protein purification procedures were carried out at 4°C. The supernatant was loaded onto a 5 ml Ni-Sepharose column equilibrated with 20 mM sodium phosphate (pH 7.6) and 500 mM NaCl (buffer A). The column was washed with 10 ml of buffer A and then with 10 ml of buffer A implemented with 5 mM imidazole. The bound proteins were eluted with 70 ml of a 0.1–0.25 M imidazole linear gradient in buffer A. The TorD protein was eluted in two peaks at 160 mM (major peak, the monomeric form) and at 240 mM imidazole (minor peak, the dimeric form). Each protein fraction was then handled independently. After dialysis against 10 mM sodium phosphate (pH 7.6) and 10 mM DTT, the TorD fractions were applied on a UnoQ6 anion exchange column (Biorad) equilibrated with 20 mM Tris-HCl (pH 8) and 10 mM DTT and eluted with a 0.075–0.4 M NaCl linear gradient in this buffer. Monomeric TorD was eluted at 150 mM NaCl, and dimeric TorD was eluted at 220 mM NaCl. Minor

contaminants in the monomeric TorD fraction were removed on a Superdex 75 column (Hiload 16/60; Pharmacia) equilibrated with 20 mM Tris-HCl (pH 8), 150 mM NaCl, and 10 mM DTT. The TorD monomers (in 20 mM Tris-HCl [pH 8], 150 mM NaCl, and 10 mM DTT) and dimers (20 mM Tris-HCl [pH 8], 220 mM NaCl, and 10 mM DTT) were concentrated to 10 mg ml^{-1} and 2.5 mg ml^{-1}, respectively, with Centricon 10 filter units (Amicon-Millipore) and stored at 4°C. The selenium-substituted protein was expressed in methionine auxotroph strain B834(DE3) with minimal medium supplemented with 17 amino acids, the bases for nucleic acids, various salts, sulfate, IPTG, and SeMet [34]. The SeMet protein was purified by the same procedure, except that all buffers were supplemented with 5 mM βME.

Crystallization

Crystallization of the TorD dimer was achieved by the hanging drop vapor diffusion method at 4°C. The crystals were obtained by mixing 1 μl (1.2 mg ml^{-1}) of protein solution with an equal volume of reservoir solution containing 1.6 M ammonium sulfate in 100 mM MES (pH 6.4). Crystals appeared in 4–6 days. They belong to space group $P2_12_12_1$, with cell parameters a = 64.3 Å, b = 95.9 Å, and c = 97.3 Å, and contain one dimer per asymmetric unit. Crystals of the selenomethionylated TorD dimers were obtained in similar conditions. Two microliters of protein solution (1.2 mg/ml in 20 mM Tris-HCl [pH 8.0], 240 mM NaCl, and 10 mM DTT) and 1 μl of reservoir solution (1.7 M ammonium sulfate and 100 mM MES [pH 6.6]) were equilibrated against 500 μl of the reservoir solution. Crystals (300 × 200 × 100 μm^3) appeared after 4–6 days at 4°C. They belong to space group $P2_12_12_1$, with cell parameters a = 66.0 Å, b = 93.4 Å, and c = 95.1 Å.

Data Collection and Phasing

MAD data collection was performed at 100 K on a single crystal of selenomethionylated protein. Before being flash-cooled in a stream of gaseous nitrogen, the crystal was cryoprotected by soaking for a few seconds in a solution of the reservoir complemented with 15% (w/v) ethylene glycol. The fluorescence spectrum, recorded before data collection on the frozen crystals, was used to select the wavelength in the selenium K absorption edge (λ_1 = 0.9787 Å, maximum of |f′|), at the peak (λ_2 = 0.9785 Å, maximum of f″), and at a high-energy remote wavelength (λ_3 = 0.9537 Å). MAD data to 2.40 Å resolution were collected on the BW7A beamline at Deutches Elektronen-Synchrotron (DESY, Hamburg, Germany), on a MarCCD detector. Diffracted intensities were measured with MOSFLM [35] and scaled and merged with SCALA [36] from the CCP4 package [37] (Table 1). Heavy-atom positions were automatically determined with SOLVE [17]. This program was also used for the refinement of the heavy-atom parameters and for phasing (Table 1). The electron density map was improved by density modification with DM [38], assuming a solvent content of 60%. Noncrystallographic symmetry averaging was not used at any stage in structure determination. The B factor determined from a Wilson plot was 41.5 $Å^2$.

Model Building and Crystallographic Refinement

The modified 2.4 Å electron density map was of sufficient quality to allow tracing of 79% of the TorD main chain and 63% of the side chain atoms. The structure was refined by the maximum likelihood method, as implemented in CNS [39], including a bulk solvent correction, intertwined with manual fitting into σ_A-weighted electron density maps [40] displayed with TURBO-FRODO [41]. All data to 2.4 Å were used in refinement, except 5% of randomly selected reflections, which were used for the calculation of the free R factor [42]. The structure was analyzed with the program PROMOTIF [43]. The coordinates have been deposited in the Protein Data Bank (accession code 1N1C).

Small-Angle X-Ray Scattering

X-ray-scattering data were collected on the small-angle instrument D24 [44] at LURE (Orsay, France) with monodisperse solutions of TorD monomer (10.7 mg/ml in 20 mM Tris-HCl buffer [pH 8.0], 300 mM NaCl, and 5 mM DTT) and TorD dimer (5.1 mg/ml in 20 mM Tris-HCl buffer [pH 8.0], 204 mM NaCl, 300 mM NaSCN, and 5 mM DTT). The data acquisition system has been described [45]. The wavelength of the X-ray was 1.488 Å (Ni K absorption edge), and the sample to detector distance was set to 1639.5 mm. All experiments were performed at 4°C with a temperature-controlled cell [46]. Eight successive frames of 200 s were collected for each sample. The scattering intensity of a reference sample of carbon black, recorded immediately before and after each experiment, was used to normalize all data to the transmitted intensity. The scattering contribution of the buffer was subtracted before further analysis. The X-ray-scattering patterns, for the dimer and for one globular module within the dimmer, were computed from crystallographic coordinates with the program CRYSOL [47].

Acknowledgments

We thank the staff at the Deutches Elektronen-Synchrotron for excellent data collection facilities. This work was financed by CNRS and, in part, by "Le Programme de Recherche en Microbiologie Fondamentale" of the French Ministry of Research.

Received: July 19, 2002
Revised: October 23, 2002
Accepted: November 14, 2002

References

1. Dos Santos, J.P., Iobbi-Nivol, C., Couillault, C., Giordano, G., and Méjean, V. (1998). Molecular analysis of the trimethylamine N-oxide (TMAO) reductase respiratory system from a Shewanella species. J. Mol. Biol. *284*, 421–433.
2. Proctor, L.M., and Gunsalus, R.P. (2000). Anaerobic respiratory growth of Vibrio harveyi, Vibrio fischeri and Photobacterium leiognathi with trimethylamine N-oxide, nitrate and fumarate: ecological implications. Environ. Microbiol. *2*, 399–406.
3. Shaw, A.L., Hanson, G.R., and McEwan, A.G. (1996). Cloning and sequence analysis of the dimethylsulfoxide reductase structural gene from Rhodobacter capsulatus. Biochim. Biophys. Acta *1276*, 176–180.
4. Mouncey, N.J., Choudhary, M., and Kaplan, S. (1997). Characterization of genes encoding dimethyl sulfoxide reductase of Rhodobacter sphaeroides 2.4.1T: an essential metabolic gene function encoded on chromosome II. J. Bacteriol. *179*, 7617–7624.
5. Barrett, E.L., and Kwan, H.S. (1985). Bacterial reduction of trimethylamine oxide. Annu. Rev. Microbiol. *39*, 131–149.
6. Gon, S., Patte, J.C., Dos Santos, J.P., and Méjean, V. (2002). Reconstitution of the trimethylamine oxide reductase regulatory elements of Shewanella oneidensis in Escherichia coli. J. Bacteriol. *184*, 1262–1269.
7. Méjean, V., Iobbi-Nivol, C., Lepelletier, M., Giordano, G., Chippaux, M., and Pascal, M.C. (1994). TMAO anaerobic respiration in Escherichia coli: involvement of the tor operon. Mol. Microbiol. *11*, 1169–1179.
8. Iobbi-Nivol, C., Pommier, J., Simala-Grant, J., Méjean, V., and Giordano, G. (1996). High substrate specificity and induction characteristics of trimethylamine-N-oxide reductase of Escherichia coli. Biochim. Biophys. Acta *1294*, 77–82.
9. Czjzek, M., Dos Santos, J.P., Pommier, J., Giordano, G., Méjean, V., and Haser, R. (1998). Crystal structure of oxidized trimethylamine N-oxide reductase from Shewanella massilia at 2.5 A resolution. J. Mol. Biol. *284*, 435–447.
10. Gon, S., Giudici-Orticoni, M.T., Méjean, V., and Iobbi-Nivol, C. (2001). Electron transfer and binding of the c-type cytochrome TorC to the trimethylamine N-oxide reductase in Escherichia coli. J. Biol. Chem. *276*, 11545–11551.
11. Gon, S., Jourlin-Castelli, C., Theraulaz, L., and Méjean, V. (2001). An unsuspected autoregulatory pathway involving apocytochrome TorC and sensor TorS in Escherichia coli. Proc. Natl. Acad. Sci. USA *98*, 11615–11620.
12. Pommier, J., Méjean, V., Giordano, G., and Iobbi-Nivol, C. (1998). TorD, a cytoplasmic chaperone that interacts with the unfolded trimethylamine N-oxide reductase enzyme (TorA) in Escherichia coli. J. Biol. Chem. *273*, 16615–16620.
13. Santini, C.L., Ize, B., Chanal, A., Muller, M., Giordano, G., and

Wu, L.F. (1998). A novel sec-independent periplasmic protein translocation pathway in Escherichia coli. EMBO J. *17*, 101–112.
14. Berks, B.C., Sargent, F., De Leeuw, E., Hinsley, A.P., Stanley, N.R., Jack, R.L., Buchanan, G., and Palmer, T. (2000). A novel protein transport system involved in the biogenesis of bacterial electron transfer chains. Biochim. Biophys. Acta *1459*, 325–330.
15. Voordouw, G. (2000). A universal system for the transport of redox proteins: early roots and latest developments. Biophys. Chem. *86*, 131–140.
16. Tranier, S., Mortier-Barrière, I., Ilbert, M., Birck, C., Iobbi-Nivol, C., Mejean, V., and Samama, J.P. (2002). Characterization and multiple molecular forms of TorD from Shewanella massilia, the putative chaperone of the molybdoenzyme TorA. Protein Sci. *11*, 2148–2157.
17. Terwilliger, T.C., and Berendzen, J. (1999). Automated MAD and MIR structure solution. Acta Crystallogr. D Biol. Crystallogr. *55*, 849–861.
18. Laskowski, R.A., MacArthur, M.W., Moss, D.S., and Thornton, J.M. (1993). PROCHECK: a program to check the stereochemical quality of protein structures. J. Appl. Crystallogr. *26*, 283–291.
19. Holm, L., and Sander, C. (1996). Mapping the protein universe. Science *273*, 595–603.
20. Schlunegger, M.P., Bennett, M.J., and Eisenberg, D. (1997). Oligomer formation by 3D domain swapping: a model for protein assembly and misassembly. Adv. Protein Chem. *50*, 61–122.
21. Oresnik, I.J., Ladner, C.L., and Turner, R.J. (2001). Identification of a twin-arginine leader-binding protein. Mol. Microbiol. *40*, 323–331.
22. Shaw, A.L., Leimkuhler, S., Klipp, W., Hanson, G.R., and McEwan, A.G. (1999). Mutational analysis of the dimethylsulfoxide respiratory (dor) operon of Rhodobacter capsulatus. Microbiology *145*, 1409–1420.
23. Nicholls, A., Sharp, K.A., and Honig, B. (1991). Protein folding and association: insights from the interfacial and thermodynamic properties of hydrocarbons. Proteins *11*, 281–296.
24. Rousseau, F., Schymkowitz, J.W., Wilkinson, H.R., and Itzhaki, L.S. (2001). Three-dimensional domain swapping in p13suc1 occurs in the unfolded state and is controlled by conserved proline residues. Proc. Natl. Acad. Sci. USA *98*, 5596–5601.
25. Bergdoll, M., Remy, M.H., Cagnon, C., Masson, J.M., and Dumas, P. (1997). Proline-dependent oligomerization with arm exchange. Structure *5*, 391–401.
26. Bourne, Y., Watson, M.H., Hickey, M.J., Holmes, W., Rocque, W., Reed, S.I., and Tainer, J.A. (1996). Crystal structure and mutational analysis of the human CDK2 kinase complex with cell cycle-regulatory protein CksHs1. Cell *84*, 863–874.
27. Raaijmakers, H., Vix, O., Toro, I., Golz, S., Kemper, B., and Suck, D. (1999). X-ray structure of T4 endonuclease VII: a DNA junction resolvase with a novel fold and unusual domain-swapped dimer architecture. EMBO J. *18*, 1447–1458.
28. Bennett, M.J., Choe, S., and Eisenberg, D. (1994). Domain swapping: entangling alliances between proteins. Proc. Natl. Acad. Sci. USA *91*, 3127–3131.
29. Steere, B., and Eisenberg, D. (2000). Characterization of high-order diphtheria toxin oligomers. Biochemistry *39*, 15901–15909.
30. Vitagliano, L., Adinolfi, S., Sica, F., Merlino, A., Zagari, A., and Mazzarella, L. (1999). A potential allosteric subsite generated by domain swapping in bovine seminal ribonuclease. J. Mol. Biol. *293*, 569–577.
31. Tegoni, M., Ramoni, R., Bignetti, E., Spinelli, S., and Cambillau, C. (1996). Domain swapping creates a third putative combining site in bovine odorant binding protein dimer. Nat. Struct. Biol. *3*, 863–867.
32. Berks, B.C., Sargent, F., and Palmer, T. (2000). The Tat protein export pathway. Mol. Microbiol. *35*, 260–274.
33. Sargent, F. (2001). A marriage of bacteriology with cell biology results in twin arginines. Trends Microbiol. *9*, 196–198.
34. Hendrickson, W.A., Horton, J.R., and LeMaster, D.M. (1990). Selenomethionyl proteins produced for analysis by multiwavelength anomalous diffraction (MAD): a vehicle for direct determination of three-dimensional structure. EMBO J. *9*, 1665–1672.
35. Leslie, A.G.W. (1987). Profile fitting. In Computational Aspects of Protein Crystal Analysis. Proceedings of the Daresbury Study Weekend, J.R. Helliwell, P.A. Machin, and M.Z. Papiz, eds. (Daresbury, UK: Daresbury Laboratory), pp. 39–50.
36. Evans, P.R. (1993). Data reduction. In Data Collection and Processing. Proceedings of the CCP4 Study Weekend, L. Sawyer, N. Isaacs, and S. Bayley, eds. (Daresbury, UK: Daresbury Laboratory), pp. 114–122.
37. CCP4 (1994). The CCP4 suite: programs for protein crystallography. Acta Crystallogr. D Biol Crystallogr. *50*, 760–763.
38. Cowtan, K. (1994). An automated procedure for phase improvement by density modification. Jt. CCP4 ESF-EACBM Newsl. Protein Crystallogr. *31*, 34–38.
39. Brunger, A.T., Adams, P.D., Clore, G.M., DeLano, W.L., Gros, P., Grosse-Kunstleve, R.W., Jiang, J.S., Kuszewski, J., Nilges, M., Pannu, N.S., et al. (1998). Crystallography and NMR system: a new software suite for macromolecular structure determination. Acta Crystallogr. D Biol. Crystallogr. *54*, 905–921.
40. Read, R.J. (1986). Improved Fourier coefficients for maps using phases from partial structures with errors. Acta Crystallogr. A *42*, 140–149.
41. Roussel, A., and Cambillau, C. (1989). TURBO-FRODO. In Silicon Graphics Geometry Partner Directory (Mountain View, CA: Silicon Graphics), pp. 71–78.
42. Brunger, A.T. (1993). Assessment of phase accuracy by cross validation: the free R value. Methods and applications. Acta Crystallogr. D Biol. Crystallogr. *49*, 24–36.
43. Hutchinson, E.G., and Thornton, J.M. (1996). PROMOTIF—a program to identify and analyze structural motifs in proteins. Protein Sci. *5*, 212–220.
44. Depautex, C., Desvignes, C., Leboucher, P., Lemonnier, M., Dagneaux, D., Benoit, J.P., and Vachette, P. (1987). LURE Annual Report 1985–1987 (Orsay, France: LURE).
45. Boulin, C., Kempf, R., Koch, M.H.J., and McLaughlin, S.M. (1986). Data appraisal, evaluation and display for synchrotron radiation experiments: hardware and software. Nucl. Instrum. Methods Phys. Res. A *249*, 399–407.
46. Dubuisson, J.M., Decamps, T., and Vachette, P. (1997). Improved signal-to-background ratio in small-angle X-ray scattering experiments with synchrotron radiation using an evacuated cell for solutions. J. Appl. Crystallogr. *30*, 49–54.
47. Svergun, D., Barberato, C., and Koch, M.H.J. (1995). CRYSOL—a program to evaluate X-ray solution scattering of biological macromolecules from atomic coordinates. J. Appl. Crystallogr. *28*, 768–773.
48. Kabsch, W., and Sander, C. (1983). Dictionary of protein secondary structure: pattern recognition of hydrogen-bonded and geometrical features. Biopolymers *22*, 2577–2637.
49. Gouet, P., Courcelle, E., Stuart, D.I., and Metoz, F. (1999). ESPript: analysis of multiple sequence alignments in PostScript. Bioinformatics *15*, 305–308.